Plating and Stripping Calcium in an Organic Electrolyte

Da Wang[1‡], Xiangwen Gao[1‡], Yuhui Chen[1], Liyu Jin[1], Christian Kuss[1] and Peter G. Bruce[1*]

[1] Departments of Materials and Chemistry, University of Oxford, Parks Road, Oxford, OX1 3PH, UK

[*] To whom correspondence should be addressed. E-mail: peter.bruce@materials.ox.ac.uk

There is considerable interest in multivalent cation batteries, such as those based on Mg, Ca or Al[1-11]. Most attention has focused on Mg. In all cases the metal anode represents a significant challenge. Recent work has shown that calcium can be plated and stripped, but only at elevated temperatures, 75 to 100 °C, with small capacities, typically 0.165 mAh cm^{-2}, and accompanied by significant side reactions[7]. Here we demonstrate that calcium can be plated and stripped at room temperature with capacities of 1 mAh cm^{-2} at a rate of 1 mA cm^{-2}, with low polarization (~ 100 mV) and in excess of 50 cycles. The dominant product is Ca, accompanied by a small amount of CaH_2 that forms by reaction between the deposited Ca and the electrolyte, $Ca(BH_4)_2$ in tetrahydrofuran (THF). This occurs in preference to the reactions which take place in most electrolyte solutions forming $CaCO_3$, $Ca(OH)_2$ and calcium alkoxides and normally terminate the electrochemistry. The CaH_2 protects the Ca metal at open circuit. While this work does not solve all the problems of calcium as an anode in calcium-ion batteries, it does demonstrate that significant quantities of calcium can be plated and stripped at room temperature with low polarization.

Lithium-ion batteries continue to dominate research effort. However, there is rapidly growing interest in multivalent-ion batteries as potential post-lithium ion energy storage devices[1-6, 9-19]. Although Mg and Ca are inferior to Li gravimetrically, volumetric capacity is important and in this regard Mg (3832 mAh cm^{-3}) and Ca (2072 mAh cm^{-3}) are respectively greater than and similar to Li (2062 mAh cm^{-3})[7]. Also, whereas Mg has a potential of 0.67 V vs. Li, Ca is much closer to Li at 0.17 V vs. Li, and Ca^{2+} mobility in cathodes may be higher than Mg^{2+} due to the lower charge density of Ca^{2+}. As a result, interest in Ca based batteries is rising rapidly, although still at the research stage and with significant research challenges to be met[7, 20-27]. The problem generally encountered with multivalent metal anodes in aprotic-based electrolytes is their tendency to reduce the solvent producing passivating layers that inhibit plating and stripping of the metal[1-4, 7, 12, 13].

Early work on Ca metal anodes demonstrated that although calcium can be stripped it requires a relatively high overpotential. Ca plating presents an even greater problem[12]. In electrolyte solutions such as those based on propylene carbonate, butyrolactone and acetonitrile, $Ca(OH)_2$, $CaCO_3$ and calcium alkoxides are typically formed during the electrochemical reduction[12]. The decomposition products soon passivate the electrode surface, inhibiting further calcium plating[7, 12]. Recent studies reported the important result that under conditions of elevated temperatures, 75 to 100 °C, and in electrolyte solutions, specifically $Ca(BF_4)_2$ in ethylene carbonate and propylene carbonate mixtures, calcium deposition is possible but with significant side reactions, including the formation of CaF_2, and with the deposition of only relatively small quantities corresponding to 0.165 mAh cm^{-2} [7].

Demonstrating that significant quantities of calcium can be deposited and stripped with low polarization at realistic rates and at room temperature, and that this can be sustained on cycling, is a challenge.

Borohydrides are strong reducing agents. $Mg(BH_4)_2$ has been investigated for Mg plating and stripping with some success, although high overpotentials are encountered, e.g. 700 mV, with low coulombic efficiencies of 40 % in tetrahydrofuran (THF) and 67 % in 1,2-Dimethoxyethane (DME). $LiBH_4$ has to be added to the electrolyte solution to aid dissociation of $Mg(BH_4)_2$ [28]. In contrast $Ca(BH_4)_2$ was found to be readily soluble in THF at room temperature[29]. Inspired by the magnesium results, we have investigated calcium plating and stripping in the relatively reducing electrolyte solutions based on $Ca(BH_4)_2$ in THF, obtaining capacities of 1 mAh cm^{-2} at a rate of 1 mA cm^{-2}, with low polarization (~100 mV) and in excess of 50 cycles.

The electrolytes were prepared and the cells constructed as described in the Methods section. Initial investigation of calcium plating and stripping in $Ca(BH_4)_2$ in THF was carried out by cyclic voltammetry (CV) using three-electrode cells, Fig. 1 a. The CV is typical for metal plating on reduction and its stripping on subsequent oxidation. A coulombic efficiency of 94.8 % is obtained from the CV. Calcium deposition starts at potentials ~ 200 mV below the thermodynamic potential for Ca/Ca^{2+}. The oxidation stability of the electrolyte solution is approx. 3V vs Ca/Ca^{2+}, Supplementary Fig. S 1 a. To investigate the calcium anode in the $Ca(BH_4)_2$ in THF electrolyte solution in more detail, three-electrode cells were constructed and subjected to galvanostatic cycling, in which the counter and reference electrodes were calcium metal. Calcium was deposited corresponding to a capacity of 1 mAh cm^{-2}, at a rate of 1 mA cm^{-2}. The variation of voltage on calcium deposition and stripping is shown in Fig. 1 b. The polarization (overpotential) on repeated plating and stripping is ~ 100 mV, with a larger overpotential of very short duration on the 1st plating, corresponding to ~ 250 mV, Fig. 1 b. The first cycle round-trip efficiency is 93 % up to the maximum oxidation potential of 0.5 V vs. Ca/Ca^{2+}. The round-trip coulombic efficiency shown in the inset to Fig. 1 b generally increases over the first 25 cycles up to 94-96 %. The achieved cycling efficiency is beyond our expectation, but still far from practical use. It is important to note that the results in Fig. 1 b require a clean glovebox atmosphere. If the atmosphere is contaminated by solvents, such as organic carbonates, the stripping polarization increases somewhat earlier than in Fig. 1 b, see Fig. S 1 b and FTIR of the working electrode shows evidence of additional peaks.

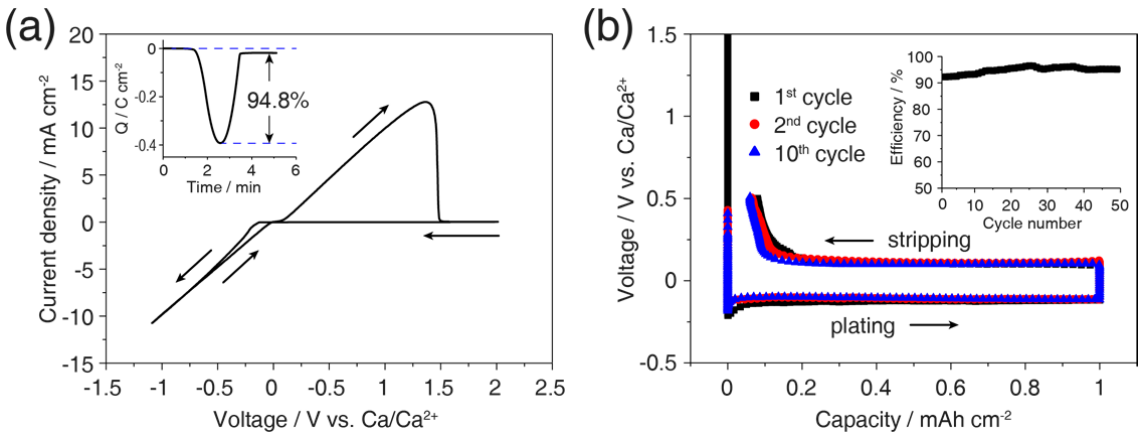

Figure 1 | Electrochemical results of Ca plating/stripping in 1.5 M $Ca(BH_4)_2$ in THF. (a) Cyclic voltammogram of Ca plating/stripping. The working, reference and counter electrodes are Au, Ca and Pt respectively. Scan

rate 25 mV s^{-1}. Inset shows charge passed on plating/stripping from the CV. (b) Galvanostatic Ca plating/stripping at the rate of 1 mA cm^{-2}. The working, reference and counter electrodes are Au, Ca and Ca respectively. The plating/stripping potentials are corrected for the IR drop across the electrolyte. Inset shows variation of coulombic efficiency with cycle number.

It is necessary to prove that these electrochemical results do represent calcium deposition. To do so, anodes were extracted from the cell after calcium deposition and the deposit on the electrode surface was collected and subjected to powder X-ray diffraction (PXRD). All procedures were carried out in an Ar atmosphere glovebox and diffraction data collected using a sample holder for air sensitive materials, see Methods section. The PXRD pattern is shown in Fig. 2 a. The dominant product is calcium metal, along with a small amount of CaH_2. To examine the possibility that non-crystalline compounds could have formed, an infrared spectrum was also collected on the material removed from the electrode surface. Fourier transform infrared (FTIR) spectrum is shown in Fig. 2 b along with a range of possible calcium oxidation products, including those observed in previous work for Ca in aprotic electrolytes[12]. The FTIR spectrum is featureless, consistent with the products being Ca and CaH_2. The $Ca(BH_4)_2$/THF electrolyte changes significantly the chemistry at the calcium/electrolyte interface from that normally encountered in Ca-based electrolytes.

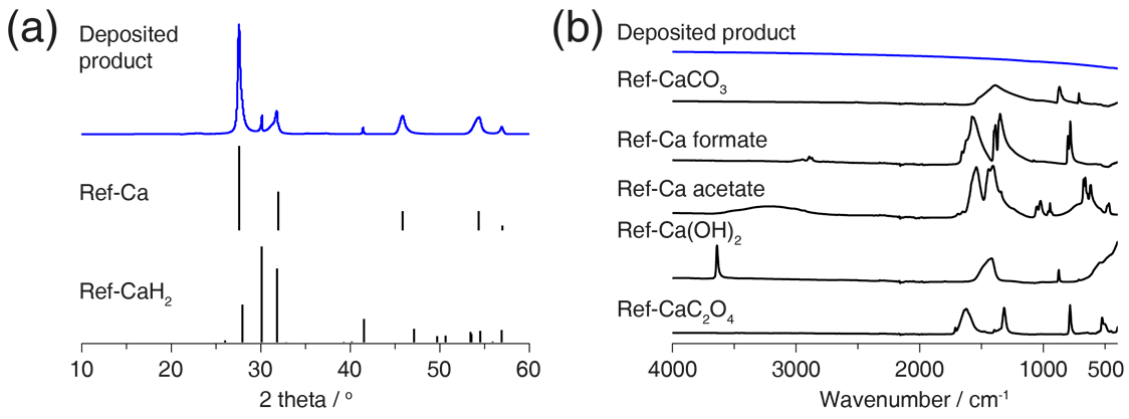

Figure 2 | Characterization of the product formed on Ca plating. (a) Powder X-ray diffraction patterns showing the dominant product on plating is Ca with a small amount of CaH_2; (b) Infrared spectra of the deposited product and common Ca oxidation products.

Presenting electrochemical data, even accompanied by proof that the dominant product of the deposition is Ca, is not sufficient. It is also necessary to quantify the amount of calcium deposited and compare it with the charge passed, in order to examine if the latter leads quantitatively to the former, i.e. to establish how close the Ca deposition comes to the theoretical ideal of 2 e^-/Ca. The quantity of Ca deposited was determined by treating the electrode with a solution of D_2SO_4 in D_2O then analysing the gases evolved by mass spectrometer. The results are shown in Supplementary Fig. S 2, in which the fluxes of the two gases evolved, D_2 and HD, are shown. D_2 and HD arise from the reactions:

$$Ca + D_2SO_4 \rightarrow D_2 + CaSO_4$$

$$CaH_2 + D_2SO_4 \rightarrow 2\ HD + CaSO_4$$

No other significant gases were detected. Integration of the curves in Supplementary Fig. S 2 for D_2 and HD respectively give the quantities of Ca and CaH_2 on the electrode, Table 1. The total amount of Ca deposited (i.e. the sum of Ca metal and CaH_2) corresponds to 98 % of the charge passed (1.828 µmol for 0.1 mAh of charge). This represents a charge/mass ratio of 2.04 e^-/Ca, demonstrating that the majority of charge passed leads to Ca deposition and not to parallel electrochemical side reactions. A small amount of the Ca deposited, 5.0 mole %, reacts with the electrolyte to form CaH_2. A similar analysis was applied to the electrode at the end of 1st and 10th stripping, Table 1. No Ca remained after the 1st stripping only some residual CaH_2, corresponding to 2.1 mole % of the total charge passed on stripping (0.093 mAh). For the electrode at the end of 10th stripping, both D_2 and HD were detected, corresponding to 4.0 mole % Ca and 6.3 mole % CaH_2 respectively. These values represent the accumulation of products rather than the cycling efficiency on the 10th cycle, which is 94 %. These results indicate that some of the CaH_2 is lost from the electrode on stripping, and not all Ca is stripped at higher cycle numbers.

Table 1 | Amounts of Ca and CaH_2 formed on plating and remaining after stripping, expressed as a mole % of the amount of charge passed in each case. The values for the amounts after the 10th stripping represent an accumulation of Ca and CaH_2 remaining on the electrode and not the cycling efficiency on the 10th cycle.

	Ca	CaH_2
After 1st plating	93.0 %	5.0 %
After 1st stripping	below detection limit	2.1 %
After 10th stripping	4.0 %	6.3 %

The morphology of the Ca was investigated by SEM, Fig. 3. A thick film of calcium is evident after the 1st plating. After stripping, some residue is left on the electrode surface, which from the above chemical analysis is CaH_2. Further cycles show the corresponding plating and stripping of the Ca film, with some residue of Ca and CaH_2 at the end of each stripping process. To investigate whether the CaH_2 exists as a layer on top of the calcium film or instead throughout the Ca film, time-of-flight secondary ion mass spec (TOF-SIMS) was carried out with depth profiling on deposited film from a deuterated THF electrolyte solution. The results are shown in Supplementary Fig. S 3. Although D^- ions were found to be more prevalent near the surface, they were also found throughout the deposited film. This result is consistent with the freshly deposited Ca reacting with the THF to form CaH_2 continuously during the electrochemical deposition of Ca, as the deuterated THF is the only source of D.

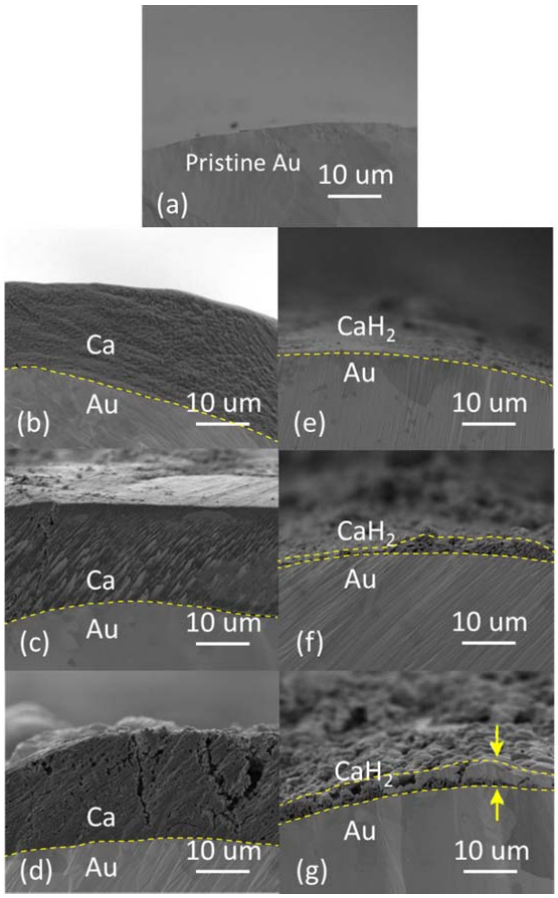

Figure 3 | Cross sectional images of Au electrodes at the end of Ca plating/stripping. The specific capacity for each plating is 1 mAh cm^{-2}. (a) Pristine Au electrode, (b) 1^{st} plating, (c) 5^{th} plating, (d) 10^{th} plating, (e) 1^{st} stripping, (f) 5^{th} stripping, (g) 10^{th} stripping.

GC-MS studies showed that Ca reacts with THF to form CaH_2 by abstracting two protons: Ca + C_4H_8O → CaH_2 + C_4H_6O, see Supplementary Information. The electrolyte salt also plays a role. Two identical cells differing only in the electrolyte salts, $Ca(BH_4)_2$ and $Ca(TFSI)_2$, were subjected to calcium plating and stripping, see Supplementary Fig. S 5. In the case of the $Ca(TFSI)_2$ the cell polarizes severely and there is almost no capacity. FTIR, Supplementary Fig. S 5 b, reveals multiple peaks, in contrast to the FTIR for the $Ca(BH_4)_2$/THF electrolyte. These results demonstrate the role of $Ca(BH_4)_2$ in avoiding side reactions between Ca and the electrolyte that would otherwise inhibit the Ca/Ca^{2+} electrochemistry. This is consistent with previous studies of calcium in THF based electrolytes using salts such as $Ca(BF_4)_2$, where decomposition products like $Ca(OH)_2$ and $Ca(OR)_2$ were observed and made plating and stripping impossible[12].

Since the reaction between Ca and the electrolyte to form CaH_2 is spontaneous, we investigated whether this reaction continues unabated or saturates. Calcium was deposited on the electrode and then left at open circuit for various periods of time. The accumulation of CaH_2 with time is shown in Fig. 4 a. After deposition of 1 mAh cm^{-2} of Ca the electrode contained, as above, 5 mole % of CaH_2 (expressed as a percentage of the total charge passed). The quantity of CaH_2 grew to 11 mole % over some 20 hours, at which point the growth of CaH_2 saturated. The CaH_2 layer on the surface of the

deposited Ca serves to protect the Ca from further reaction with the electrolyte at open circuit. SEM images show the appearance of a film on the surface of the deposited Ca, Fig.4 b, which is not evident immediately after deposition, Fig. 3 b.c.d. These results indicate that CaH_2 grows by reaction with Ca as it deposits, and is therefore distributed throughout the film, but then on resting at open circuit the growth of CaH_2 continues until a protective film of CaH_2 forms of sufficient thickness to suppress further reaction between Ca and the electrolyte solution. An overpotential of several hundred millivolts at a current density of 1 mA cm^{-2} is required to initiate stripping after the electrode has been standing at open circuit, compared with stripping immediately after the deposition, see Supplementary Fig. S 6 a. Also the round-trip efficiency has been reduced, commensurate with the greater accumulation of CaH_2 on standing. Another consequence of the CaH_2 formation is a lower round-trip efficiency at lower current densities (longer exposure of growing Ca film to the electrolyte). This is shown in Supplementary Fig. S 6 b, where the round-trip efficiency has dropped from 94 % to 90 % when plating/stripping was carried out at 0.1 mA cm^{-2}.

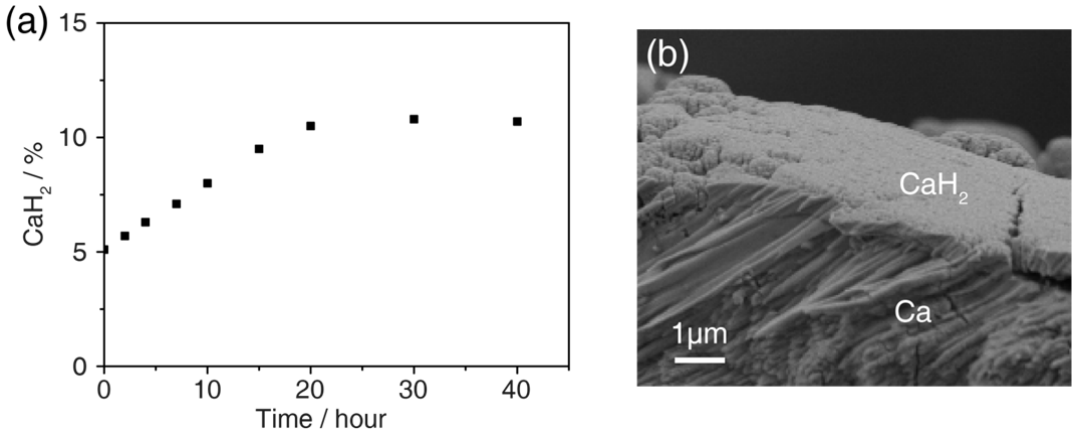

Figure 4 | Accumulation of CaH_2 on deposited electrode. (a) Accumulation of CaH_2 at open circuit after depositing 1 mAh cm^{-2} of Ca on the electrode, expressed as a mole percentage of the charge passed. (b) Cross sectional image of electrode after 20 hours rest at open circuit.

Outlook

All previous attempts to plate and strip calcium have met with the formation of decomposition products due to reaction with the electrolyte that either makes calcium plating and stripping impossible or requires elevated temperatures to achieve even relatively low plating capacities. In contrast, using the electrolyte $Ca(BH_4)_2$/THF it is possible to plate and strip calcium at room temperature and in significant quantities (1 mAh cm^{-2}), with low polarisation (100 mV) with efficiencies of approx. 94-96 % and on continuous cycling. With $Ca(BH_4)_2$ in THF, instead of forming the usual products of calcium oxidation, CaH_2 forms, and this changes significantly the Ca electrochemistry. From the above studies, we know that CaH_2 forms spontaneously during calcium deposition and is included within the growing calcium film. The formation is relatively slow compared with the rate of plating and stripping. Only at open circuit, where there is no calcium deposition to compete with CaH_2 formation, do we see a CaH_2 film form on the calcium surface. Even so, the stripping can still be initiated with an overpotential of several hundred millivolts. Therefore, CaH_2, the by-product of Ca plating/stripping in $Ca(BH_4)_2$/THF electrolyte, unlike the usual products of Ca oxidation, does not inhibit plating and stripping, but instead forms a protection layer at open circuit, sufficient to inhibit continuous calcium reaction with the electrolyte.

Although the results reported here represent a significant advance in the plating and stripping of Ca in an organic based electrolyte, they do not solve the problems of the Ca anode for rechargeable Ca batteries. The cycling efficiency of a metal anode for rechargeable batteries needs to be as high as 99.98% per cycle. The cycling efficiency here, although high at 96%, is not sufficient for such practical applications. Ca is reactive. To achieve 99.98% cycling efficiency it would be necessary to form a SEI layer on Ca that is electronically insulating but Ca^{2+} conducting. In the present work, Ca reacts with THF to form CaH_2 which acts as a passivating layer at open circuit, mitigating further reaction of Ca with the electrolyte. However this does not have the properties of a SEI and hence does not support sufficiently high efficiency. The cathode is another challenge for the Ca battery. Generally the diffusivity of divalent ions in intercalation hosts is relatively slow, which can limit practical rates, although the lower charge density of Ca^{2+} compared with Mg^{2+} makes, all other things being equal, Ca^{2+} mobility greater than Mg^{2+}. It is particularly difficult to find high voltage Ca intercalation hosts with high Ca^{2+} mobility because the more polarizable hosts, e.g. sulphides and nitrides, are limited to lower voltages than the less polarizable oxides. The oxidation stability of the $Ca(BH_4)_2$/THF electrolyte solution, Supplementary Fig. S 1 a, is approx. 3V vs Ca/Ca^{2+}, which limits possible cathodes to relatively low voltage the Chevrel phases[24], V_2O_5[15] and sulfur[20]. The redox potential of Prussian Blue and its derivatives[21, 25, 30], which have been investigated recently for use in multivalent-ion batteries is too high. The combination of a Ca anode with the borohydride/ether based electrolytes and cathodes that are within the stability window may be of interest for primary batteries.

Methods

Please refer to the Supplementary Information for details of the Materials and Methods.

References

1. Muldoon J., Bucur C. B., Gregory T. Quest for Nonaqueous Multivalent Secondary Batteries: Magnesium and Beyond. *Chem Rev*, **114,** 11683-11720 (2014).

2. Aurbach D., Lu Z., Schechter A., Gofer Y., Gizbar H., Turgeman R*., et al.* Prototype systems for rechargeable magnesium batteries. *Nature*, **407,** 724-727 (2000).

3. Yoo H. D., Shterenberg I., Gofer Y., Gershinsky G., Pour N., Aurbach D. Mg rechargeable batteries: an on-going challenge. *Energ Environ Sci*, **6,** 2265-2279 (2013).

4. Muldoon J., Bucur C. B., Oliver A. G., Sugimoto T., Matsui M., Kim H. S*., et al.* Electrolyte roadblocks to a magnesium rechargeable battery. *Energ Environ Sci*, **5,** 5941-5950 (2012).

5. Hayashi M., Arai H., Ohtsuka H., Sakurai Y. Electrochemical characteristics of calcium in organic electrolyte solutions and vanadium oxides as calcium hosts. *J Power Sources*, **119,** 617-620 (2003).

6. Lin M. C., Gong M., Lu B. G., Wu Y. P., Wang D. Y., Guan M. Y.*, et al.* An ultrafast rechargeable aluminium-ion battery. *Nature*, **520,** 324-328 (2015).

7. Ponrouch A., Frontera C., Barde F., Palacin M. R. Towards a calcium-based rechargeable battery. *Nat Mater*, **15,** 169-172 (2016).

8. Tepavcevic S., Slater M., Johnson C. S., Rajh T. Nanostructured layered cathode for Mg-ion batteries. *Abstr Pap Am Chem S*, **245,** (2013).

9. Kaveevivitchai W., Manthiram A. High-capacity zinc-ion storage in an open-tunnel oxide for aqueous and nonaqueous Zn-ion batteries. *J Mater Chem A*, **4,** 18737-18741 (2016).

10. Wang R. Y., Shyam B., Stone K. H., Weker J. N., Pasta M., Lee H. W.*, et al.* Reversible Multivalent (Monovalent, Divalent, Trivalent) Ion Insertion in Open Framework Materials. *Adv Energy Mater*, **5,** (2015).

11. Okoshi M., Yamada Y., Komaba S., Yamada A., Nakai H. Theoretical Analysis of Interactions between Potassium Ions and Organic Electrolyte Solvents: A Comparison with Lithium, Sodium, and Magnesium Ions. *J Electrochem Soc*, **164,** A54-A60 (2017).

12. Aurbach D., Skaletsky R., Gofer Y. The Electrochemical-Behavior of Calcium Electrodes in a Few Organic Electrolytes. *J Electrochem Soc*, **138,** 3536-3545 (1991).

13. Xu K. Electrolytes and Interphases in Li-Ion Batteries and Beyond. *Chem Rev*, **114,** 11503-11618 (2014).

14. Gofer Y., Chusid O., Gizbar H., Viestfrid Y., Gottlieb H. E., Marks V.*, et al.* Improved electrolyte solutions for rechargeable magnesium batteries. *Electrochem Solid St*, **9,** A257-A260 (2006).

15. Tepavcevic S., Liu Y. Z., Zhou D. H., Lai B., Maser J., Zuo X. B.*, et al.* Nanostructured Layered Cathode for Rechargeable Mg-Ion Batteries. *Acs Nano*, **9,** 8194-8205 (2015).

16. Canepa P., Gautam G. S., Hannah D. C., Malik R., Liu M., Gallagher K. G.*, et al.* Odyssey of Multivalent Cathode Materials: Open Questions and Future Challenges. *Chem Rev*, **117,** 4287-4341 (2017).

17. Kaveevivitchai W., Huq A., Manthiram A. Microwave-assisted chemical insertion: a rapid technique for screening cathodes for Mg-ion batteries. *J Mater Chem A*, **5,** 2309-2318 (2017).

18. Yu X. W., Manthiram A. Performance Enhancement and Mechanistic Studies of Magnesium-Sulfur Cells with an Advanced Cathode Structure. *Acs Energy Lett*, **1,** 431-437 (2016).

19. Keyzer E. N., Glass H. F. J., Liu Z. G., Bayley P. M., Dutton S. E., Grey C. P*., et al.* Mg(PF6)(2)-Based Electrolyte Systems: Understanding Electrolyte-Electrode Interactions for the Development of Mg-Ion Batteries. *J Am Chem Soc*, **138,** 8682-8685 (2016).

20. See K. A., Gerbec J. A., Jun Y. S., Wudl F., Stucky G. D., Seshadri R. A High Capacity Calcium Primary Cell Based on the Ca-S System. *Adv Energy Mater*, **3,** 1056-1061 (2013).

21. Tojo T., Sugiura Y., Inada R., Sakurai Y. Reversible Calcium Ion Batteries Using a Dehydrated Prussian Blue Analogue Cathode. *Electrochimica Acta*, **207,** 22-27 (2016).

22. Amatucci G. G., Badway F., Singhal A., Beaudoin B., Skandan G., Bowmer T*., et al.* Investigation of yttrium and polyvalent ion intercalation into nanocrystalline vanadium oxide. *J Electrochem Soc*, **148,** A940-A950 (2001).

23. Wang R. Y., Wessells C. D., Huggins R. A., Cui Y. Highly Reversible Open Framework Nanoscale Electrodes for Divalent Ion Batteries. *Nano Lett*, **13,** 5748-5752 (2013).

24. Smeu M., Hossain M. S., Wang Z., Timoshevskii V., Bevan K. H., Zaghib K. Theoretical investigation of Chevrel phase materials for cathodes accommodating Ca2+ ions. *J Power Sources*, **306,** 431-436 (2016).

25. Padigi P., Goncher G., Evans D., Solanki R. Potassium barium hexacyanoferrate - A potential cathode material for rechargeable calcium ion batteries. *J Power Sources*, **273,** 460-464 (2015).

26. Padigi P., Kuperman N., Thiebes J., Goncher G., Evans D., Solanki R. Calcium Cobalt Hexacyanoferrate Cathodes for Rechargeable Divalent Ion Batteries. *Journal of New Materials for Electrochemical Systems*, **19,** 57-64 (2016).

27. Shiga T., Kondo H., Kato Y., Inoue M. Insertion of Calcium Ion into Prussian Blue Analogue in Nonaqueous Solutions and Its Application to a Rechargeable Battery with Dual Carriers. *J Phys Chem C,* **119,** 27946-27953 (2015).

28. Mohtadi R., Matsui M., Arthur T. S., Hwang S. J. Magnesium Borohydride: From Hydrogen Storage to Magnesium Battery. *Angew Chem Int Edit*, **51,** 9780-9783 (2012).

29. Borisov A. P., Makhaev V. D. Preparation of Calcium Cyclopentadienyl Complexes Using Calcium Borohydride. *Russ Chem B+*, **42,** 339-340 (1993).

30. Kuperman N., Padigi P., Goncher G., Evans D., Thiebes J., Solanki R. High performance Prussian Blue cathode for nonaqueous Ca-ion intercalation battery. *J Power Sources*, **342,** 414-418 (2017).

Acknowledgements

PGB is indebted to the EPSRC including SUPERGEN for financial support. We acknowledge Gareth Llewellyn and Dr. James Wickens for the GC-MS experiments.

Author Contributions

‡These authors contributed equally to this work. D.W. and X. G. designed experiments and performed electrochemical studies and characterization. D.W., X. G., Y. C., L. J., C. K. and P.G.B analysed and interpreted the data. P.G.B. wrote the manuscript.

Competing financial interests

The authors declare no competing financial interests.

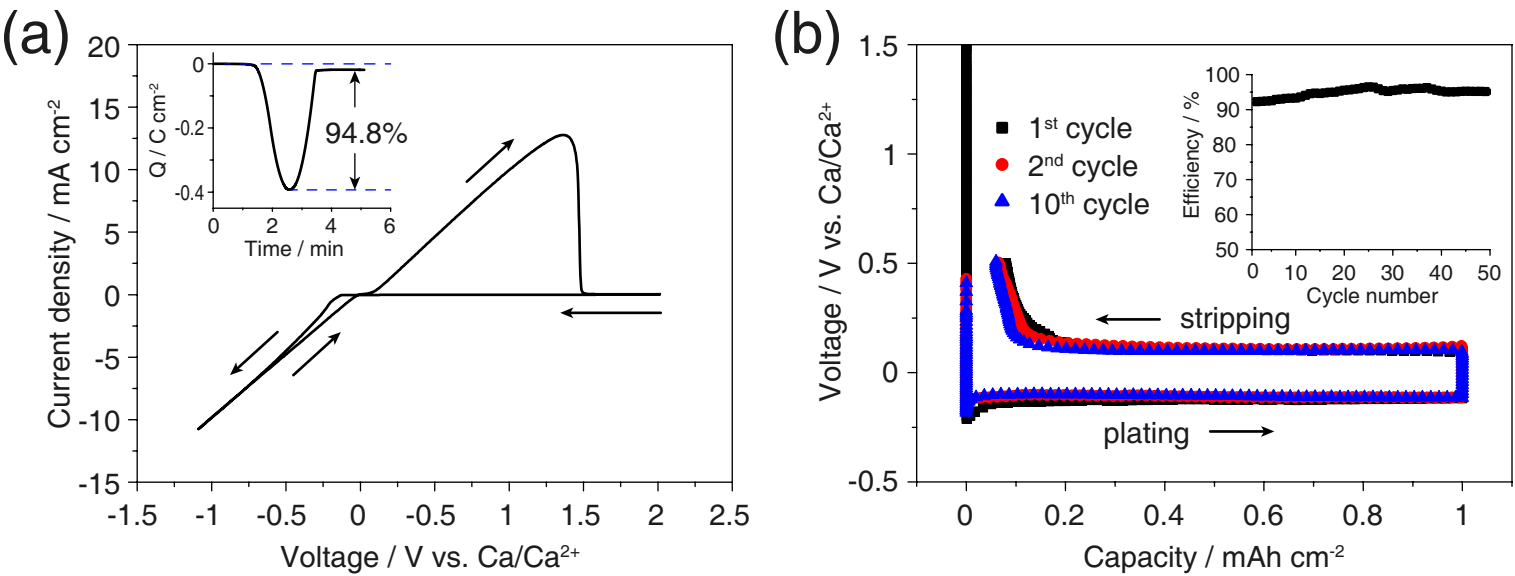
(a)
Current density / mA cm-2
Voltage / V vs. Ca/Ca2+
Q / C cm-2
Time / min
94.8%
(b)
Voltage / V vs. Ca/Ca2+
Capacity / mAh cm-2
1st cycle
2nd cycle
10th cycle
stripping
plating
Efficiency / %
Cycle number

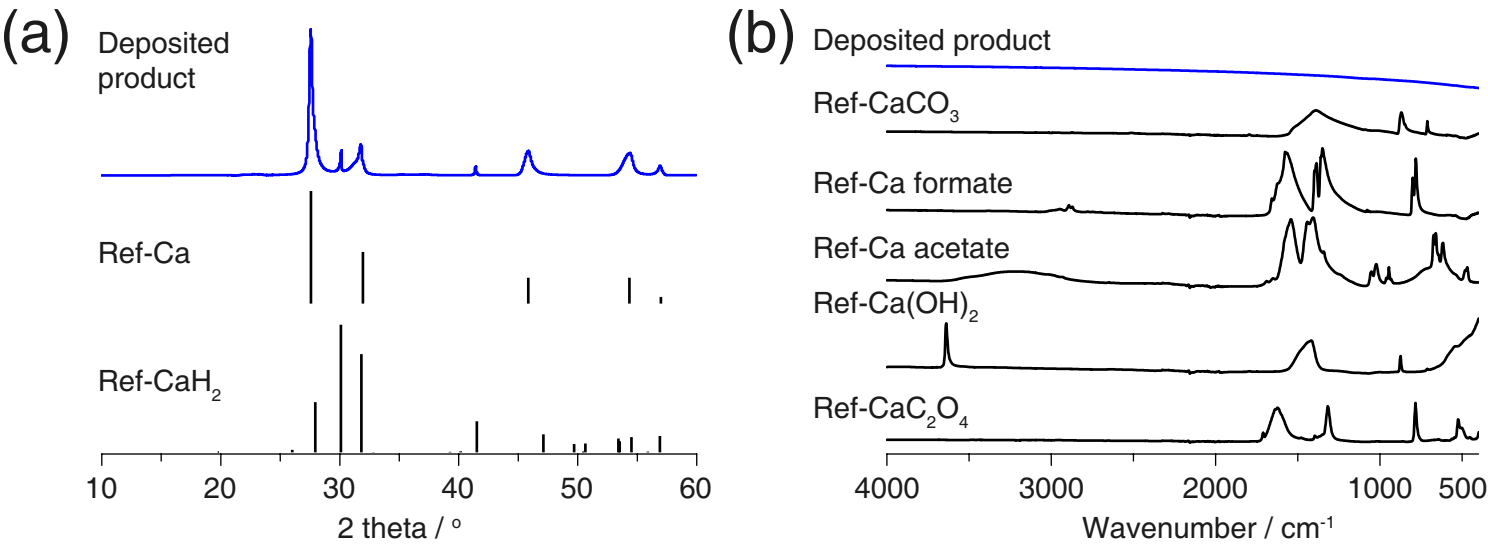
(a)
Deposited product
Ref-Ca
Ref-CaH2
10
20
30
40
50
60
2 theta / °
(b)
Deposited product
Ref-CaCO3
Ref-Ca formate
Ref-Ca acetate
Ref-Ca(OH)2
Ref-CaC2O4
4000
3000
2000
1000
500
Wavenumber / cm-1

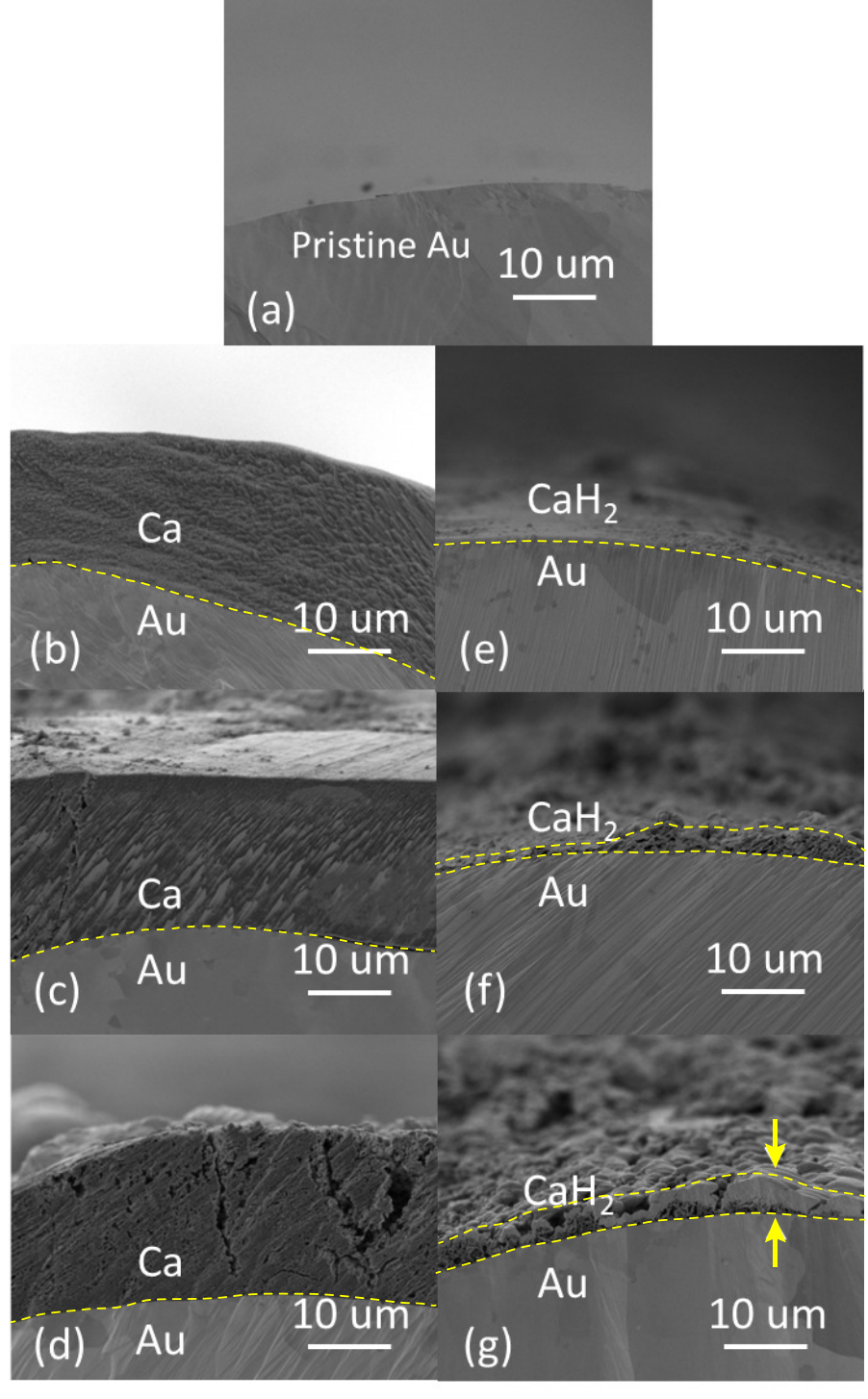
Pristine Au
10 um
(a)
Ca
Au
10 um
(b)
Ca
Au
10 um
(c)
Ca
Au
10 um
(d)
CaH2
Au
10 um
(e)
CaH2
Au
10 um
(f)
CaH2
Au
10 um
(g)

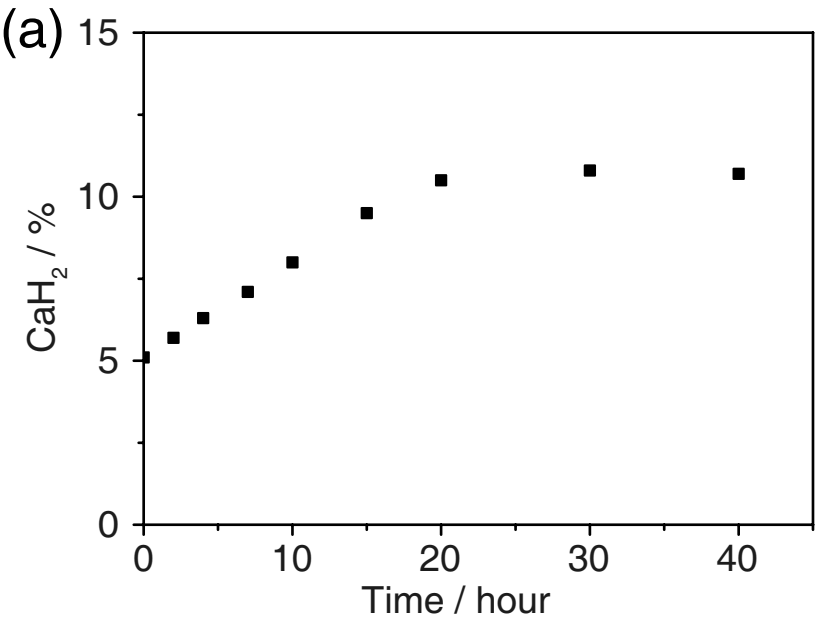
(a)
15
10
5
0
CaH2 / %
0
10
20
30
40
Time / hour

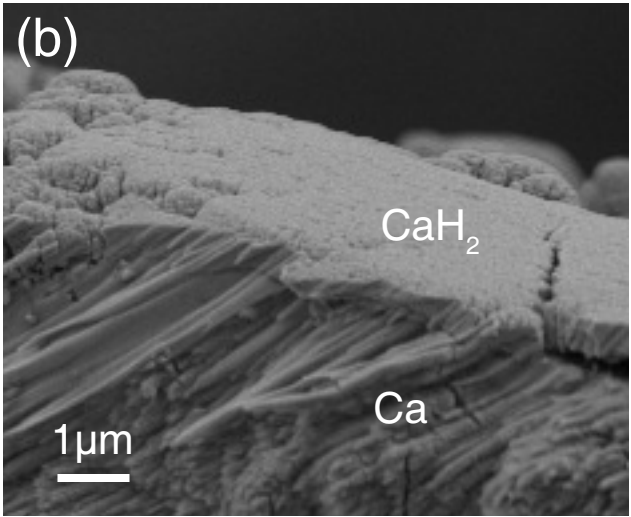
(b)
CaH2
Ca
1μm